Characterization of 3D PET systems for accurate quantification of myocardial blood flow

Renaud, Jennifer M.[1]; Yip, Kathy[2]; Guimond, Jean[3]; Trottier, Mikaël[3]; Pibarot, Philippe[3]; Turcotte, Eric[4]: Maguire, Conor[5]; Lalonde, Lucille[5]; Gulenchyn, Karen[6]; Farncombe, Troy[6]; Wisenberg, Gerald[7]; Moody, Jonathan[8]; Lee, Benjamin[8]; Port, Steven C.[9]; Turkington, Timothy G.[10], Beanlands, Rob S.[1]; deKemp, Robert A.[1]

[1]National Cardiac PET Centre, University of Ottawa Heart Institute, Ottawa ON, Canada
[2]KMH Cardiology & Diagnostic Centre, Mississauga ON, Canada
[3]Institut Universitaire de Cardiologie et de Pneumologie de Québec, QC, Canada
[4]Centre Hospitalier Universitaire de Sherbrooke, QC, Canada
[5]University of Alberta Hospital, Edmonton AB, Canada
[6]St Joseph's Healthcare, Hamilton ON, Canada
[7]Lawson Health Research Institute, London ON, Canada
[8]INVIA Medical Imaging Solutions, Ann Arbor MI, U.S.A
[9]Aurora Cardiovascular Services, Milwaukee WI, U.S.A
[10]Duke University Medical Center, Durham NC, U.S.A

Research article: Dynamic range is defined as a scanner-specific maximum injected activity/body-weight, below which myocardial blood flow can be quantified accurately using Rb-82 3D-PET imaging.

First author:
Jennifer Renaud, MSc   Tel: +1.613.798.5555 x16417
National Cardiac PET Centre   Fax: +1.613.761.4929
University of Ottawa Heart Institute   Email: jrenaud@ottawaheart.ca
40 Ruskin St., Room H-1206
Ottawa, Ontario K1Y 4W7

Corresponding author:
Robert deKemp, PhD   Tel: +1.613.761.4275
Room H-1215, *same as above*   Fax: +1.613.761.4929
                                             Email: radekemp@ottawaheart.ca

Word count: 5000

Running foot line: PET dynamic range for MBF quantification

ABSTRACT

Three-dimensional (3D) mode imaging is the current standard for positron emission tomography-computed tomography (PET-CT) systems. Dynamic imaging for quantification of myocardial blood flow (MBF) with short-lived tracers, such as Rb-82-chloride (Rb-82), requires accuracy to be maintained over a wide range of isotope activities and scanner count-rates. We propose new performance standard measurements to characterize the dynamic range of PET systems for accurate quantitative imaging. **Methods**: 1100-3000 MBq of Rb-82 or N-13-ammonia was injected into the heart wall insert of an anthropomorphic torso phantom. A decaying isotope scan was performed over 5 half-lives on 9 different 3D PET-CT systems and 1 3D/two-dimensional (2D) PET-only system. Dynamic images (28x15s) were reconstructed using iterative algorithms with all corrections enabled. Dynamic range was defined as the maximum activity in the myocardial wall with <10% bias, from which corresponding dead-time, count-rates and/or injected activity limits were established for each scanner. Scatter correction residual bias was estimated as the maximum cavity blood-to-myocardium activity ratio. Image quality was assessed via the coefficient of variation measuring non-uniformity of the left ventricle (LV) myocardium activity distribution. **Results**: Maximum recommended injected activity/body-weight, peak dead-time correction factor, count-rates and residual scatter bias for accurate cardiac MBF imaging were: 3-14 MBq/kg, 1.5-4.0, 22-64 Mcps singles and 4-14 Mcps prompt coincidence count-rates, and 2-10% on the investigated scanners. Non-uniformity of the myocardial activity distribution varied from 3-16%. **Conclusion**: Accurate dynamic imaging is possible on the 10 3D-PET systems if the maximum injected MBq/kg values are respected to limit peak dead-time losses during the bolus first-pass transit.

Key Words: dynamic range; cardiac positron emission tomography; rubidium-82.

INTRODUCTION

PET imaging in 3D-mode has become the standard for new whole-body scanners. The increased sensitivity allows for reduction of injected activity to the patient while maintaining excellent image quality; however, random and scattered photon counts are increased, requiring systems with high count-rate capability and accurate corrections for these physical effects. Current PET instrumentation and National Electrical Manufacturers Association (NEMA) performance evaluation methods (*1*) have been developed primarily to optimize whole-body oncology imaging with F-18 FDG. However, dynamic PET imaging for MBF quantification with short-lived tracers, such as Rb-82, O-15-water or N-13-ammonia, requires high count-rates and correction accuracy to be maintained over a wide range of measured activities (*2*). An ideal PET system should allow for conventional relative myocardial perfusion imaging (MPI) of tracer retention without compromising accuracy of first-pass dynamic data (*3*). Routine MBF imaging is clinically feasible with the 76s half-life generator-produced tracer Rb-82, resulting in accurate (*4,5*) and reproducible measurements (*3,6-8*), as validated against N-13-ammonia and O-15-water standards (*9-12*).

We propose methods to evaluate the dynamic operating range of 3D PET systems for quantitative imaging of MBF. Patient imaging protocols were implemented and used to confirm the predicted operating range.

MATERIALS AND METHODS

Phantom Scans

Image Acquisition. Rb-82 decaying isotope scans were performed over 5 half-lives using an anthropomorphic torso phantom (model ECT/TOR/P; Data Spectrum Corp.),

approximating a small male upper torso (38x26 cm) (*13*) on 8 different 3D PET-CT systems and 1 3D/2D PET-only system. An N-13-ammonia scan was performed on 1 other 3D PET-CT camera (Supplemental Table 1). The phantom contained a myocardial heart cavity and wall insert (model ECT/CAR/I; Data Spectrum Corp.), lungs, spine and liver chamber (Figs. 1A and B). Liver and body cavities were filled with water to mimic soft tissue attenuation. The phantom was placed in prone position in the PET field-of-view to facilitate infusion directly into the myocardial wall, and 1500-3000 MBq (40-80 mCi) of Rb-82, or 1100 MBq of N-13-ammonia was infused. Rb-82 was infused either as a 30s 'square-wave' with saline push, or as 50 mL/min 'bolus' (Supplemental Table 1). A list-mode PET acquisition was started immediately after completion of tracer infusion, simulating the localized activity and high count-rate observed during tracer first-pass transit through the heart. For attenuation correction, the PET scan was followed by a low-dose CT scan on the PET-CT systems or a 4-minute transmission scan on the PET-only camera.

Image Reconstruction. Dynamic images (28 frames x 15s) were reconstructed using vendor-supplied Fourier rebinning-filtered backprojection or iterative expectation-maximization algorithms (*14*), with an 8mm or 12mm Hann or Gaussian post-filter and all corrections enabled for isotope decay, attenuation, scatter, randoms, prompt-gammas, detector efficiency and dead-time, according to routine clinical practice at each institution. Most systems had explicit prompt-gamma correction enabled during reconstruction (Supplemental Table 1); others used a 50cm CT attenuation correction field-of-view to minimize the contribution of prompt-gamma photons to the 3D coincidence background (*15*).

Quantitative Analysis. Reconstructed image time-activity curves (TAC) were analyzed to determine the dynamic operating range where quantitative accuracy was maintained. Total injected activity TACs were measured using Inveon Research Workplace software (Siemens) (Figs. 1C and D). A spherical volume-of-interest (10cm diameter) encapsulating the activity in the heart insert was drawn (Fig. 1C) from which total decay-corrected activity, $A_{heart}(t)$ (MBq), was measured for all mid-frame scan times, t (min). From the TAC, the average decay-corrected activity in the late time-frames, where tracer uptake had reached a stable maximum, was determined as the true reference value, A_{ref} (MBq). Activity bias in each time frame was then calculated as:

$$ActivityBias(t) = (A_{heart}(t) / A_{ref} - 1) \times 100 \quad (\%) \quad\quad\quad [1]$$

To compare dynamic range among scanners ActivityBias(t) was plotted as a function of total activity in the heart volume-of-interest, $A_{decay}(t)$, where:

$$A_{decay}(t) = A_{ref} \times e^{-\lambda t} \quad (MBq) \quad\quad\quad [2]$$

For Rb-82 and N-13-ammonia, the isotope decay constants are $\lambda = \ln(2)/1.27$ and $\ln(2)/10$ (min) respectively. The time, T_{max}, of the earliest frame with ≤10% activity bias was identified (Fig. 1D) and total heart activity at $t = T_{max}$ was calculated as:

$$A_{max} = A_{heart}(T_{max}) \times e^{-\lambda T_{max}} \quad (MBq) \quad\quad\quad [3]$$

Dead-time correction factors (DTF) and prompt coincidences and/or singles count-rates associated with A_{max} were tabulated as available in the image headers. The maximum weight-based activity recommended for patient studies was estimated as A_{max} divided by 50kg, the representative body-weight of the torso phantom, determined according to the attenuating cross-sectional area, which is approximately 2.3 times larger than the NEMA scatter phantom previously shown to represent a 21.5 kg patient (*16*). A repeat scan was performed on the Discovery 690, 600, and the Biograph PET-CT-16 systems to assess reproducibility of injected activity/body-weight values.

Scatter correction residual bias was estimated as the LV cavity blood-to-myocardium ratio by plotting ScatterBias(t) as a function of $A_{decay}(t)$, where:

$$ScatterBias(t) = (C_{cavity}(t) / C_{myo}(t)) \times 100 \quad (\%) \qquad [4]$$

$C_{cavity}(t)$ represents average activity concentration in the heart cavity (Bq/cc) and $C_{myo}(t)$ is the average concentration in the myocardial wall (Bq/cc). Residual bias is an indicator of uncorrected scatter in the LV cavity and is important to measure because accurate scatter correction is required for quantitative MBF measurements using an image-derived input function. To extract myocardium and LV cavity blood TACs, our in-house FlowQuant© software was used (*3*). The blood-to-myocardium ratio was determined by taking the median of the cavity, base and atrium TACs and then dividing by the myocardium average TAC.

Image quality was assessed as non-uniformity of the myocardium activity distribution, using the coefficient of variation (COV) of the LV polar-map:

$$C_{myo}(t)_{COV} = SD_{myo}(t) / C_{myo}(t) \times 100 \quad (\%) \qquad [5]$$

$SD_{myo}(t)$ is the standard deviation of the activity concentration in the myocardial wall polar-map. Images were also inspected visually for count-rate-dependent pile-up artifacts.

Patient Scans

Patient Population. Recommended weight-based activity and DTF limits defined by the phantom scans were validated using Rb-82 PET images from 20 patients acquired on the Discovery 690 and 600, and the Scintron 3D PET cameras (Supplemental Table 2). All patients were referred for a clinically indicated myocardial perfusion scan for coronary artery disease diagnosis and/or risk stratification. The institutional review board

(or equivalent) at each of the participating centers approved this study and all subjects signed a written informed consent.

Image Acquisition. On the Discovery cameras, the Rb-82 rest scan was followed by a dipyridamole stress scan, whereas regadenoson stress was used on the Scintron. Injected activity of 10 MBq/kg body-weight was prescribed for patients scanned on the Discovery systems, and 8 MBq/kg on the Scintron, according to local clinical practice for MPI. At rest and stress, 6 minute list-mode acquisitions were started at the time of injection to capture the first-pass transit of the tracer as required for MBF quantification (Supplemental Fig. 1).

Quantitative Analysis. DTFs were tabulated for each time frame to identify the peak count-rates and dead-time losses. Global LV MBF values were computed automatically using FlowQuant©, as described for phantom scans. Blood and LV myocardium TACs were used as input to a 1-tissue compartment model with a constant distribution volume to estimate MBF (*4,6*).

Statistical Analysis

Values are presented as mean ± standard deviation. Where applicable, means were compared via the Student's t-test or one-way analysis of variance (ANOVA) using SPSS Statistics 23 (IBM). $P<0.05$ was considered statistically significant.

RESULTS

Phantom Scans

Figure 1D shows the bias in measured activity as a function of time (t) and total activity in the heart phantom insert, $A_{decay}(t)$, for a single scanner. The highest activity, A_{max}, with <10% bias was 325 MBq. Assuming a representative phantom mass of 50kg, the highest recommended patient-equivalent injected activity/body-weight was estimated as 6.5 MBq/kg. At this activity (frame 12 @2.75 min=T_{max}) the peak prompt and singles count-rates, and DTF were: 4.1 and 29 Mcps, and 2.0, respectively (Table 1).

Across all investigated scanners, the maximum recommended injected activity/body-weight, peak DTF and count-rate for accurate dynamic, quantitative cardiac MBF imaging varied between 3-14.4 MBq/kg, 1.5-4.0 DTF, 22-64 Mcps singles and 4-14 Mcps prompt count-rate, respectively (Table 1). As expected, scanners using optimized detector crystals (higher atomic number, shorter decay time, higher light output (17)) and/or improved processing electronics were found to accommodate higher injected activity/body-weight while remaining quantitatively accurate (Fig. 2). Peak DTF values within the accurate range corresponded typically with peak coincidence dead-times ≤50%. Peak count-rates varied considerably between scanners and inter-comparison was not possible in all cases, depending on the camera-specific information available. Repeat scans were within 4±9% of the originally tabulated injected activity/body-weight values (Discovery 690: 13.1 MBq/kg (+6.8%), Discovery 600: 5.7 MBq/kg (-6.4%), and Biograph PET-CT-16: 6.9 MBq/kg (+11.0%)) demonstrating good reproducibility of the proposed methodology.

Residual scatter bias varied from 2-10% within the accurate operating range (Table 1). Highly variable uncorrected scatter was observed for all scanners in early time frames when counts tend to pile-up towards the center of the detector blocks (Fig. 3A). Within the accurate operating range only, scatter bias stabilized at a relatively constant

level (Fig. 3B). This bias was found to be slightly higher on the lutetium oxyorthosilicate (LSO) detector-based systems (7.8±2.0) versus the other scanners (2.9±1.1; $p<0.05$), suggesting that the scatter correction methods implemented on these four LSO-based scanners may benefit from further optimization to improve accuracy.

All phantom images showed high contrast and low noise over the entire range of activity. Assessment of the LV myocardium polar-map non-uniformity demonstrated that COV was highest (lowest image quality) in early frames ($t=0$-T_{max}: $C_{myo}(t)_{COV}=10.2\pm4.9\%$) (Fig. 4A). COV values stabilized within the recommended operating range ($t=T_{max}$-7 min: $C_{myo}(t)_{COV}=8.9\pm3.4\%$; $p=NS$ vs. early frames) (Fig. 4B), corresponding with the trend observed for residual scatter bias. These results suggest that despite high dead-time losses in the early time frames, image quality is not compromised and is not a limiting factor for quantitative accuracy. Visual image inspection confirmed the absence of any obvious count-rate-dependent pile-up artifacts for all PET systems.

Patient Scans

Delivered activity was 10.3±0.3 and 9.9±2.0 MBq/kg for patients imaged on the Discovery 690 and 600 systems. Peak DTF values were 1.5±0.1 and 2.1±0.2 (corresponding to 33% and 50% coincidence dead-time, respectively), similar to the recommended maxima suggested by the phantom scans (Table 1). For patients scanned on the Scintron with 8 MBq/kg, peak DTF was 1.6±0.2 (38% coincidence dead-time), slightly lower than the phantom maximum value recommended to remain within the accurate dynamic operating range.

DISCUSSION

This study established methods to evaluate the accurate dynamic operating range of 3D PET systems for quantitative cardiac imaging with Rb-82. Decaying isotope phantom scans were performed over 5 half-lives to determine the optimal operating range, defined by the maximum injected activity/body-weight, and corresponding maximum singles, prompt coincidence count-rates and/or peak dead-time factors. Patient scans were performed near the suggested limits on 3 representative scanners and confirmed validity of the phantom scan recommendations. Evaluation of the scatter correction bias confirmed the effectiveness of manufacturer-implemented scatter corrections in 3D-mode. Finally, LV polar-map non-uniformity, and the absence of count-rate dependent pile-up artifacts, was found to be adequate for diagnostic evaluation.

The results suggest that the evaluated PET scanners should be able to perform accurate quantitative imaging despite differences in manufacturing technology, including: scintillation detectors, detector block size, coincidence processing hardware and prompt-gamma correction availability. The most important factor to consider for quantitative imaging in patients is that peak dead-time, singles and/or prompt coincidence count-rates remain below the threshold values determined from the phantom scans to obtain accurate images and prevent a biased MBF estimation. This technique allows for prospective determination of image accuracy, as opposed to retrospective evaluation of detector block saturation and/or other performance metrics after acquisition is completed (*18*). It can also be performed retrospectively as long as count-rate and/or dead-time parameters are contained in the image header files generated by the scanners. As opposed to the NEMA count-rate performance standard that is designed for whole-body oncology imaging, the proposed method measures myocardial activity using a more realistic cardiac imaging geometry, and the residual scatter fraction and myocardial

image uniformity are measured at the highest count-rates typically encountered during the bolus first-pass.

It is important to note that scan header information obtained from most of the scanners did not include complete count-rate and dead-time information, which would make it impossible to retrospectively verify that patient scans were obtained within the accurate operating range, and therefore that quantitative MBF values were absolutely reliable. It would be beneficial if all manufacturers recorded this information in the scan headers to allow consistent evaluation of quantitative imaging performance.

Clinical implications

An optimal PET imaging system should allow for conventional MPI and absolute MBF imaging with a single injection of tracer. For PET cameras with adequate dynamic range and where the injected activity/body-weight limit is high enough to obtain diagnostic quality perfusion images, both static MPI and dynamic MBF images can be obtained with a single injection protocol. In our previous multi-centre study, 10 MBq/kg was the benchmark established for diagnostic-quality MPI using 3D PET systems (*15*). If this threshold was applied to the cameras in the current study, a single injection protocol could be recommended on the first 4 systems listed in Table 1; the others would require a dual injection protocol to first obtain diagnostic quality perfusion images using a high-dose injection and then accurate images for MBF assessment with a lower-dose scan. However, all systems showed maintained image quality in the early frames outside of the accurate range, as measured by COV, suggesting that the dynamic range may be extended with vendor improvements in dead-time correction accuracy, potentially allowing for a single injection protocol on additional systems.

If a single injection protocol is used on a system without sufficient dynamic range, MBF values would be inaccurate since peak blood and myocardium activities would be underestimated due to high dead-time losses at activity values exceeding the dynamic range of the camera. A patient example demonstrating this effect is shown in Figure 5. A 170 cm, 100 kg female patient was scanned at rest on the Discovery 600 PET/CT system with an injected dose of 10MBq/kg Rb-82, above the maximum limit for accurate quantification determined by the phantom scan, and a 5-fold lower dose of 2 MBq/kg, for comparison. At 10 MBq/kg, the peak DTF and prompt count-rates were 2.5 and 6.8 Mcps, exceeding the recommended limits of 2.0 and 4.1 Mcps, suggesting that the camera was not operating in the accurate dynamic range for that portion of the scan. As a result, the early peak values of the blood and LV myocardium TACs are underestimated compared to the low-dose TACs (Fig. 5A). Under-estimation of the area under the blood curve causes over-estimation of the MBF values, as shown in the LV myocardium polar-maps (Fig. 5B).

Patient Scan Variability

To estimate the maximum weight-based activity to use for patient studies, A_{max} was divided by the representative weight of the phantom, estimated as 50kg. A scanner-dependent estimate based on DTF values obtained using a particular activity/body-weight protocol may be more appropriate. The patient data required to perform this estimate were available for the Discovery 690, 600 and Scintron 3D. The peak DTF values from the patient scans vary according to body-weight (Fig. 6A), therefore for each scanner the phantom DTF curve was plotted as a function of the weight-based dose (MBq/kg), using representative phantom weights corresponding with (passing through) the mean and maximum patient DTF values (Fig. 6B). Adjustment of the representative phantom weight improves prediction of the recommended injected dose for a range of

12

patient sizes, and also accounts for differences in absolute calibration between the PET scanner and rubidium elution system (used to measure the phantom and patient injected activities, respectively); the difference in calibration was relatively small (−6% to +20%) between the RUBY-FILL® (Jubilant DraxImage Inc.) elution system and Discovery scanners, whereas the difference was much larger (−68%) between the CardioGen-82® (Bracco Diagnostics Inc.) infuser and Scintron scanner. Based on the combined results, slightly lower injected activities of 9, 7 and 6 MBq/kg for the Discovery 690, 600 and Scintron would be required to keep all patient DTF values within the accurate operating range. For other scanners, the recommended injected activity/body-weight values should be confirmed or adjusted using similar methods.

Comparison with previous studies

In previous work by Tout et al. (*18*), the dynamic range of the Biograph mCT for simultaneous Rb-82 MPI and MBF assessment was investigated in patients. They determined that a dose of 1110 MBq (30 mCi) resulted in lower detector block saturation (1%) versus the manufacturer-recommended dose of 1480 MBq (40 mCi) (15% saturation). All patients were injected with the same activity rather than the weight-based dosing proposed here. Using the weight-based value of 14.4 MBq/kg determined in the present study for this scanner model and the mean weight of 87 kg from the population used in Tout et al., an average injected activity of 1250 MBq would be recommended, similar to their suggested value of 1110 MBq. As we have previously presented (*19*), administered activity can be adjusted for patient weight to compensate for the tracer distribution volume in the body and increased attenuation. Diagnostic image quality would likely be improved with the use of higher doses in larger patients, whereas smaller patients would benefit from lower radiation dose with maintained image quality. Most importantly in smaller patients, a standard dose may exceed the scanner dynamic range

during the bolus first-pass and prevent accurate MBF quantification. The method of Tout et al. relies on verifying detector block saturation post-hoc, which is not possible in real-time during patient scanning and is a more complex procedure than simple observation of the peak DTF and/or system count-rates during the patient scan.

Recently, Kolthammer et al. (20) investigated the dynamic range of the Ingenuity TF, the successor to the Gemini TF evaluated in the present study. A cylinder phantom was infused with 4 separate doses of Rb-82, ranging from 370 to 1480 MBq, with a 10-minute PET acquisition starting simultaneously with the infusion. Dynamic images were reconstructed into 15s time frames. From this experiment, they determined that Rb-82 imaging was accurate up to a peak singles count-rate of 65 Mcps at an injected activity of 925 MBq. For an average-sized patient of 70 kg, 925 MBq corresponds to an injected activity/body-weight of approximately 13 MBq/kg. For the Gemini TF investigated in the present study, we obtained a maximum recommended activity of ~5 MBq/kg, suggesting that the Ingenuity TF may accommodate higher injected activities due to improved detector crystals (lutetium-yttrium oxyorthosilicate) and electronics. As the singles count-rates were not stored in the Gemini TF header files these values could not be compared to the Ingenuity TF scanner.

In another recent study, O'Doherty et al. (21) investigated the effect of scanner dead-time on MBF values obtained from kinetic modeling of N-13-ammonia dynamic images acquired on the Discovery 710 PET/CT scanner. They showed that global LV MBF values in 4 patients were 8.9 ± 0.6 % higher when the LV blood pool input function was corrected for high dead-time losses in the early frames using the percentage difference between measured vs. true activity obtained from phantom studies. These

preliminary results again demonstrate the importance of using appropriate camera-specific maximum injected activity levels to obtain accurate MBF assessments.

CONCLUSION

Dynamic imaging to obtain accurate quantitative MBF measurements with Rb-82 appears feasible on the ten 3D PET systems evaluated when the recommended peak dead-time, maximum count-rates and injected activity limits are respected. Patient scans confirmed the validity of the injected activity/body-weight recommendations to achieve accurate and reliable quantitative images.

ACKNOWLEDGEMENTS

REFERENCES

1. National Electrical Manufacturers Association, Performance Measurements of Positron Emission Tomographs, NEMA Standards Publication NU2-2012, NEMA, Rosslyn, VA, 2013.

2. deKemp RA, Yoshinaga K, Beanlands RSB. Will 3-dimensional PET-CT enable the routine quantification of myocardial blood flow? *J Nucl Cardiol.* 2007;14:380-97.

3. Klein R, Renaud JM, Ziadi MC, et al. Intra- and inter-operator repeatability of myocardial blood flow and myocardial flow reserve measurements using rubidium-82 pet and a highly automated analysis program. *J Nucl Cardiol.* 2010;17:600-616.

4. Lortie M, Beanlands RS, Yoshinaga K, et al. Quantification of myocardial blood flow with 82Rb dynamic PET imaging. *Eur J Nucl Med Mol Imaging.* 2007;34:1765-1774.

5. Prior JO, Allenbach G, Valenta I, et al. Quantification of myocardial blood flow with 82Rb positron emission tomography: clinical validation with 15O-water. *Eur J Nucl Med Mol Imaging.* 2012;39:1037-47.

6. Efseaff M, Klein R, Ziadi MC, Beanlands RS, deKemp RA. Short-term repeatability of resting myocardial blood flow measurements using Rb-82 PET imaging. *J Nucl Cardiol.* 2012;19:997-1006.

7. deKemp RA, Declerck J, Klein R, et al. Multisoftware reproducibility study of stress and rest myocardial blood flow assessed with 3D dynamic PET/CT and a 1-tissue-compartment model of 82Rb kinetics. *J Nucl Med.* 2013;54:571-7.

8. Nesterov SV, Deshayes E, Sciagra R, et al. Quantification of myocardial blood flow in absolute terms using (82)Rb PET imaging: the RUBY-10 Study. *JACC Cardiovasc Imaging.* 2014;7:1119-27.

9. Katoh C, Yoshinaga K, Klein R, et al. Quantification of regional myocardial blood flow estimation with three-dimensional dynamic rubidium-82 PET and modified spillover correction model. *J Nucl Cardiol.* 2012;19:763-74.

10. Yoshinaga K, Manabe O, Katoh C, et al. Quantitative analysis of coronary endothelial function with generator-produced 82Rb PET: comparison with 15O-labelled water PET. *Eur J Nucl Med Mol Imaging.* 2010;37:2233-41.

11. Renaud JM, DaSilva JN, Beanlands RS, deKemp RA..Characterizing the normal range of myocardial blood flow with (82)rubidium and (13)N-ammonia PET imaging. *J Nucl Cardiol.* 2013;20:578-91.

12. El Fakhri G, Kardan A, Sitek A, et al. Reproducibility and accuracy of quantitative myocardial blood flow assessment with (82)Rb PET: comparison with (13)N-ammonia PET. *J Nucl Med.* 2009;50:1062-71.

13. Anthropomorphic Torso Phantom™ specification sheet. Data Spectrum Corporation website. http://www.spect.com/pub/Anthropomorphic_Torso_Phantom.pdf. Updated June 29, 2008. Accessed Nov. 9, 2015.

14. Hudson HM, Larkin RS. Accelerated image reconstruction using ordered subsets of projection data. *IEEE Trans Med Imaging.* 1994;13:601-9.

15. Renaud JM, Mylonas I, McArdle B, et al. Clinical interpretation standards and quality assurance for the multicenter PET/CT trial rubidium-ARMI. *J Nucl Med.* 2014;55:58-64.

16. Watson CC, Casey ME, Bendriem B, et al. Optimizing injected dose in Clinical PET by accurately modeling the counting-rate response functions specific to individual patient scans. *J Nucl Med.* 2005;46:1825-1834.

17. Melcher CL. Scintillation crystals for PET. *J Nucl Med.* 2000;41:1051-55.

18. Tout D, Tonge CM, Muthu S, Arumugam P. Assessment of a protocol for routine simultaneous myocardial blood flow measurement and standard myocardial perfusion imaging with rubidium-82 on a high count rate positron emission tomography system. *Nucl Med Commun.* 2012;33:1202-11.

19. Klein R, Beanlands RSB, deKemp RA. Quantification of myocardial blood flow and flow reserve: technical aspects. *J Nucl Cardiol.* 2010;17:555-570.

20. Kolthammer JA, Su KH, Grover A, Narayanan M, Jordan DW, Muzic RF. Performance evaluation of the Ingenuity TF PET/CT scanner with a focus on high count-rate conditions. *Phys Med Biol.* 2014;59:3843-59.

21. O' Doherty J, Schleyer P, Pike L, Marsden P. Effect of scanner dead time on kinetic parameters determined from image derived input functions in 13N cardiac PET. *J Nucl Med.* 2014;55:605.
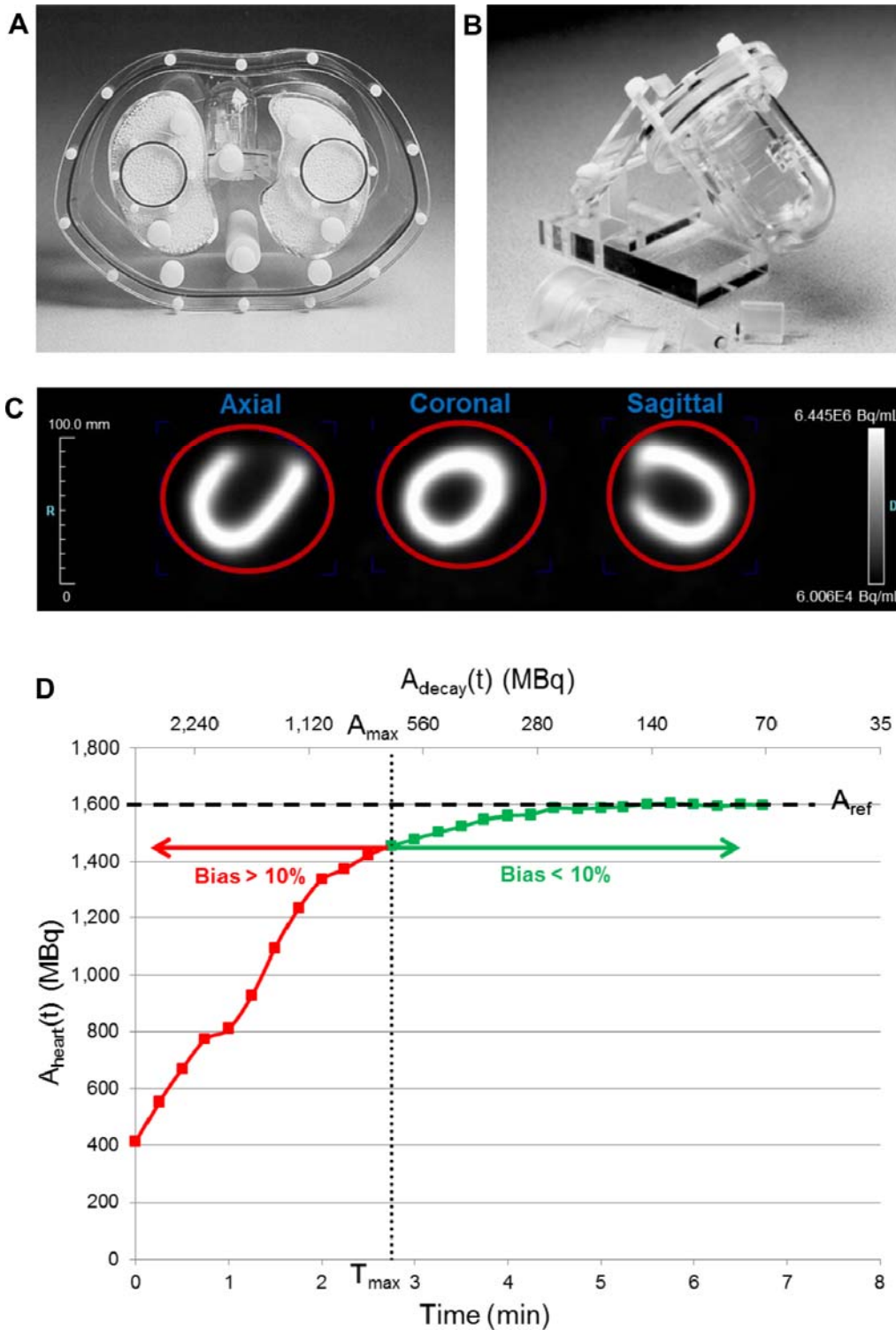
Figure 1. (A) Anthropomorphic torso phantom, including **(B)** a cardiac insert, simulating a small male patient. **(C)** Volume-of-interest (red) drawn over the entire cardiac insert and **(D)** resultant TAC. The dashed (horizontal) line indicates the reference activity value (A_{ref}). The dotted (vertical) line denotes the threshold (A_{max},T_{max}) between accurate and inaccurate quantitative values.
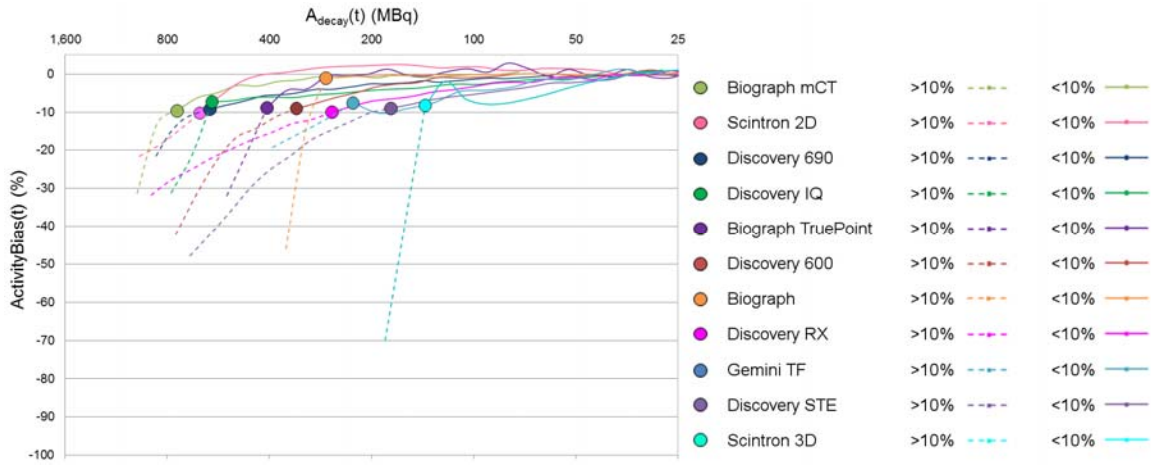
Figure 2. Total heart activity, $A_{decay}(t)$ (MBq), versus bias, ActivityBias(t) (%). Dotted lines denote activity >10% bias, while solid lines represent activity <10% bias. The highest activity with ≤10% bias, A_{max}, (circles) indicates the maximum amount of activity that can be injected while maintaining quantitatively accurate values.
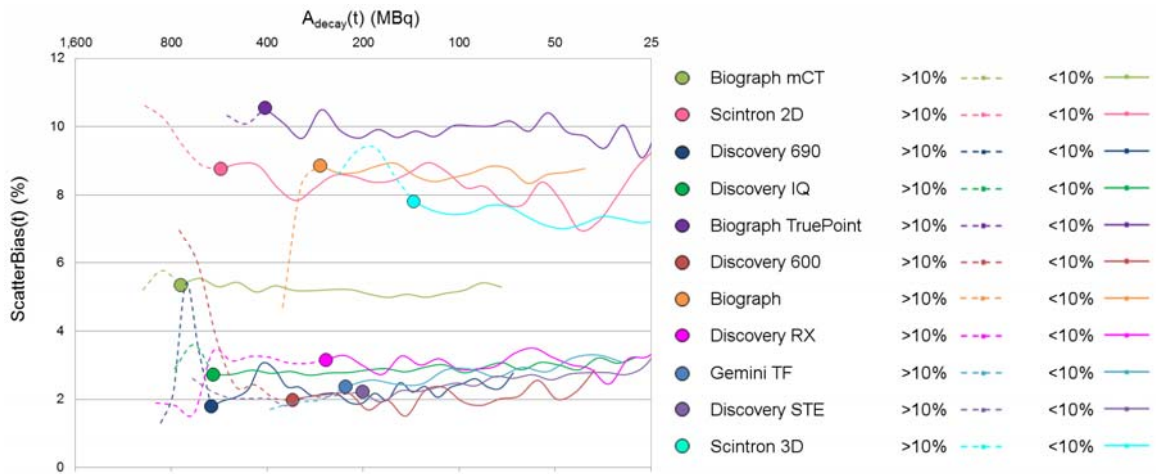
Figure 3. LV cavity blood-to-myocardium ratio plots of residual scatter. In early frames where activity is high enough to saturate the detectors (activity bias >10%) (dotted lines), there is highly variable residual scatter, **(B)** which stabilizes in the accurate range of operation (<10% bias) (solid lines).
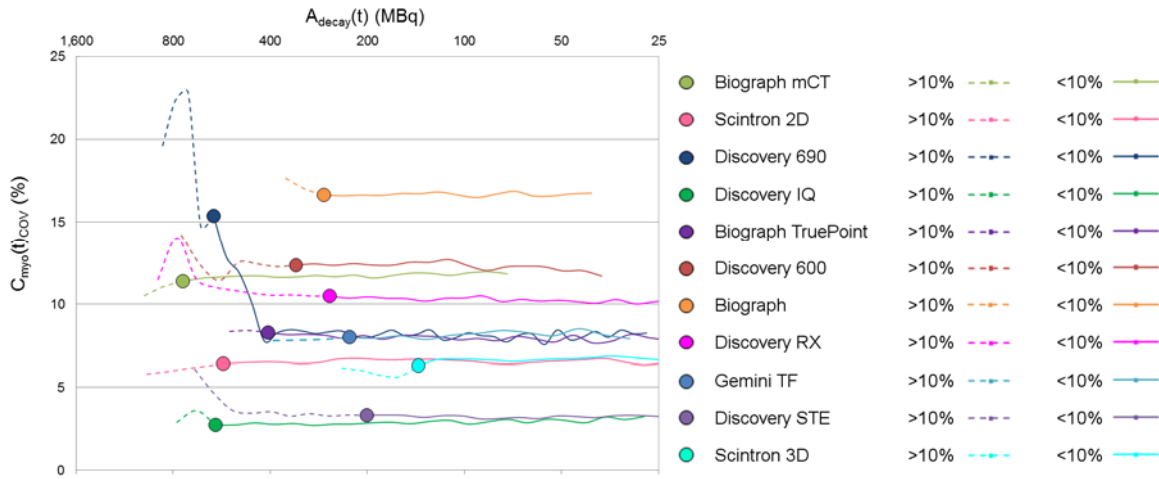
Figure 4. LV myocardium polar-map non-uniformity (COV). Outside the accurate operating range (bias >10% in early frames) the COV is highly variable (dotted lines), whereas it reaches a relatively constant level within the accurate operating range (solid lines).
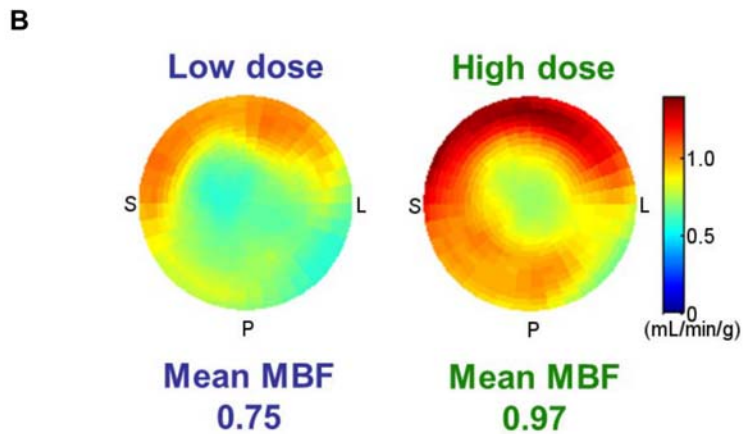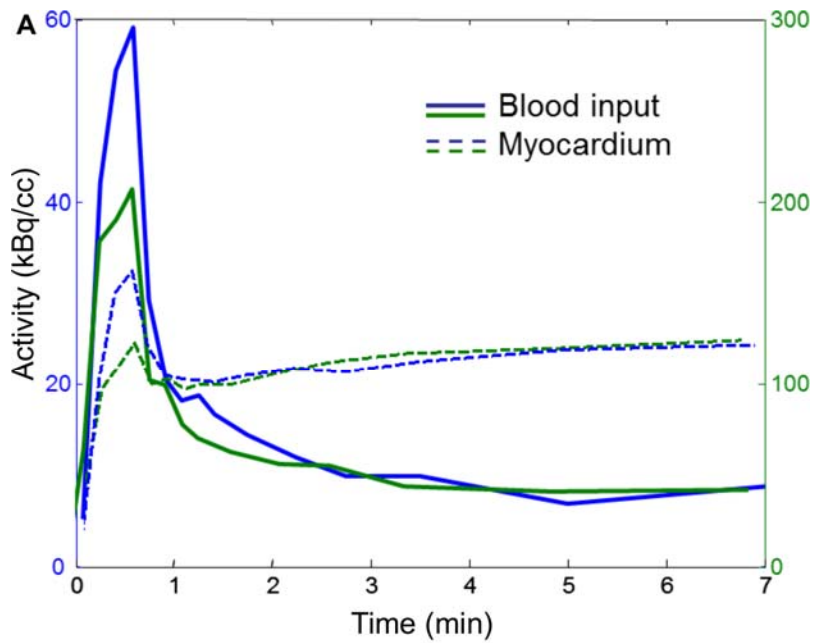
Figure 5. MBF results for a patient scanned on the Discovery 600 PET-CT system. **(A)** Blood and myocardium TACs for an injected activity/weight of 2MBq/kg (227MBq/101kg) (blue) and 10MBq/kg (1022MBq/101kg) (green). At 10 MBq/kg, peak blood and myocardium activities are under-estimated, **(B)** resulting in over-estimation of the LV myocardium MBF values. (*S, P* and *L* denote septal, posterior and lateral LV walls).
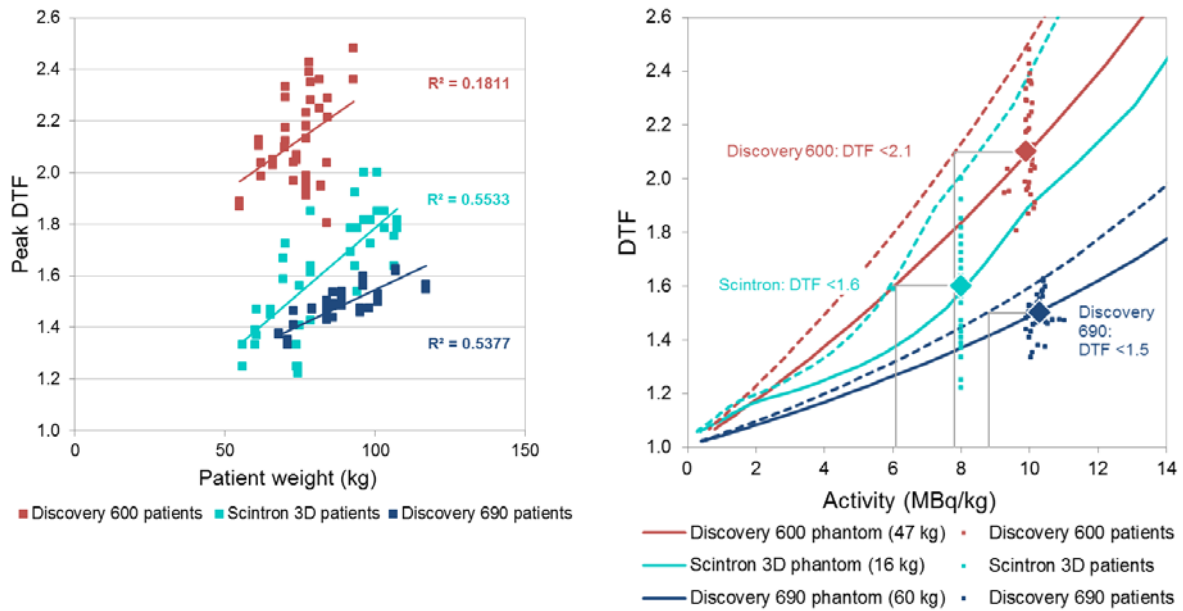
Figure 6. (A) Patient peak DTF varies with body-weight. **(B)** Similarly, peak (first-pass) DTFs increase as a function of injected activity/weight for phantom scans (solid lines). Using clinical MPI doses of 10 MBq/kg for patients on the Discovery 690 and 600 systems and 8 MBq/kg on the Scintron, mean DTF values (1.5±0.1, 2.1±0.2, 1.6±0.2; large diamonds) agreed with the recommended phantom-determined limits. Adjusted phantom curves (dashed lines) show that to ensure all patient scans remain below the maximum recommended peak DTF values, lower injected activities would be required (gray lines) since. The wider DTF distribution in patients on the Discovery 600 and Scintron may reflect higher randoms rates measured with bismuth germanium oxide and early-generation LSO detectors, compared to the lutetium-based scintillator detectors on the 690. As activity increases, bismuth germanium oxide systems produce much higher, more variable, random coincidences due to the wider coincidence time window.

Table 1. Recommended maximum injected activity and performance metrics

PET System	Patient A_{max}/weight (MBq/kg)	Peak Prompts (Mcps)	Peak Singles (Mcps)	Peak DTF	Scatter Bias(t) (%)	$C_{myo}(t)_{cov}$ (%)
Biograph mCT PET-CT-40	14.4	6.3	64	-	5.2 ± 0.2	12.4 ± 2.1
ECAT Accel Scintron PET 2D	11.4	1.6	26	1.7	8.3 ± 0.6	6.5 ± 0.2
Discovery 690 PET-VCT-64	11.4	5.9	45	1.5	2.4 ± 0.3	11.0 ± 4.8
Discovery IQ (5 ring) PET-CT-16	11.3	14.1	84	3.9	2.7 ± 1.1	2.9 ± 0.2
Biograph TruePoint PET-CT-16	8.0	-	-	-	9.9 ± 0.4	8.0 ± 0.3
Discovery 600 PET-CT-16	6.5	4.1	29	2.0	2.1 ± 0.3	12.1 ± 1.1
Biograph PET-CT-16	5.5	-	22	-	8.6 ± 0.2	16.4 ± 1.3
Discovery RX PET-CT-16	5.1	4.5	-	1.7	3.1 ± 0.3	10.6 ± 0.8
Gemini TF PET-CT-16	4.6	-	-	-	2.5 ± 0.5	7.8 ± 0.9
Discovery STE-VCT-16	3.9	3.5	-	2.1	2.5 ± 0.4	4.3 ± 3.3
ECAT Accel Scintron PET 3D	2.7	1.6	22	1.7	7.4 ± 0.2	6.5 ± 0.3

- : not available in the image header files.